Adsorption (2014) 20:649–656
DOI 10.1007/s10450-014-9611-2

A fully consistent experimental and molecular simulation study of methane adsorption on activated carbon

Fadi Khaddour · Auriane Knorst-Fouran · Frédéric Plantier · Manuel M. Piñeiro · Bruno Mendiboure · Christelle Miqueu

Received: 3 October 2013 / Revised: 7 March 2014 / Accepted: 1 April 2014 / Published online: 13 April 2014

Abstract The adsorption of pure methane in activated carbon Ecosorb was studied by combining grand canonical ensemble Monte Carlo molecular simulations and an experimental approach based on a gravimetric device. Experimental and calculated adsorption isotherms of methane were determined in supercritical conditions at 303.15 and 353.15 K and pressures up to 10 MPa. The comparison between both experimental and estimated data proves the consistency of the methodology used in this work, starting from the characterization of the porous media in terms of pore size distribution, the determination of the experimental adsorption isotherms, and the final estimation of computational results through estimated isotherms determination. Moreover, additional differential enthalpy of adsorption calculations were compared with experimental values obtained by means of a manometric/calorimetric technique. The good agreement shows the strength and the originality of this paper by combining experimental and computational homemade results allowing a complete characterization of the activated carbon substrate and its methane storage capacity.

Keywords Methane adsorption · Activated carbon · Gravimetric method · Molecular simulation

F. Khaddour · A. Knorst-Fouran · F. Plantier · B. Mendiboure · C. Miqueu (✉)
Laboratoire des Fluides Complexes et leurs Réservoirs (LFC-R), UMR 5150, CNRS, TOTAL, Univ Pau & Pays Adour, BP 1155, 64013 Pau, France
e-mail: christelle.miqueu@univ-pau.fr

M. M. Piñeiro
Departamento de Física Aplicada, Facultade de Ciencias, Universidade de Vigo, 36310 Vigo, Spain

1 Introduction

Physical adsorption of supercritical gases on porous solids and more precisely on microporous materials represents an area of investigation of great interest for many research groups. Indeed the experimental or theoretical knowledge of adsorption properties (adsorption isotherms or differential heat of adsorption, for instance) is very useful in many applications such as storage of natural gas (Matranga et al. 1992) and hydrogen (Yang et al. 2013), enhanced coalbed methane recovery (Zhou et al. 2013) and carbon dioxide sequestration (Santillán-Reyes and Pfeiffer 2011). The adsorbate–adsorbent interactions responsible of the adsorption mechanism are the key of this phenomenon, and additionally the nature of the porous material (shape and conditioning, pore size distribution (PSD) and specific area) has a crucial importance. Activated carbons can be outlined as excellent adsorbent candidates for the above mentioned applications, because of their high adsorption capacity and low cost. Many studies, especially in the 1990s, have been conducted so far to characterize both the intrinsic properties of activated carbons and their storage capacity. For instance, Quinn and co-workers have studied methane adsorption and storage capacities on several carbonaceous materials (MacDonald and Quinn 1995; Quinn and Ragan 2000; Lozano-Castelló et al. 2002a, b), Cracknell et al. (1993) have shown the influence of pore geometry on the design of microporous materials for methane storage and Chen et al. (1997) have studied the effect of the solid representation on the simulation of methane adsorption in microporous carbons. However, literature is really scarce when it comes to compare experimental and computational results of both amount adsorbed and differential heat of adsorption determined exactly in the same pressure–temperature conditions. For

instance, Abdul Razak et al. (2013) have made this experimental–theoretical comparison for isotherm adsorptions of methane and ethylene on graphitized thermal carbon black without dealing with heat of adsorption. Aukett et al. (1992) did it for methane and ethylene on AX21 but according to a most recent work of Birkett and Do (2006) their calculation of heat of adsorption is not correct.

With this aim in mind, this work is the first part of an ongoing research program, and here we focus on methane as model adsorbate to study experimentally and theoretically its adsorption on Ecosorb activated carbon under supercritical conditions, before further considering more complex systems, as for instance mixtures of different gases.

The paper is organized as follows. First, a detailed description of the gravimetric device and the method used to determine the amount adsorbed is presented, emphasizing the calibration procedure and the experimental uncertainty determination. In a second theoretical section, we recall the basis of Grand Canonical ensemble Monte Carlo (GCMC) molecular simulation technique to compute either adsorption isotherms and differential heat of adsorption. Finally, a comparison between experimental and computational results is performed at 303.15 and 353.15 K, and pressures up to 10 MPa.

2 Experimental section

2.1 Material

The Ecosorb activated carbon used as adsorbent material in this study was kindly supplied by JACOBI. The adsorbate, CH_4, as well as the calibrating gas, He, were provided by Linde Gas with a minimum declared purity of 99.995 and 99.999 % respectively.

The main characteristics of the activated carbon were determined on a Micromeritics ASAP 2020 System. The PSD was determined by a low-pressure nitrogen adsorption isotherm at 77 K (from 5×10^{-7} to 0.99 P/P_0 in relative pressure range) and evaluated by a homemade filling pressure model (Malheiro et al. 2014). As shown in Fig. 1, this activated carbon is microporous. The BET specific surface is 1,290 ± 30 $m^2\ g^{-1}$ and the average micropore volume is 0.6 $cm^3\ g^{-1}$.

2.2 Experimental setup

The adsorption measurements were performed by means of a magnetic suspension balance (Rubotherm, Germany), which, besides the excess adsorbed amount, allows the simultaneous determination of the fluid density. A sketch of the equipment setup is shown in Fig. 2.

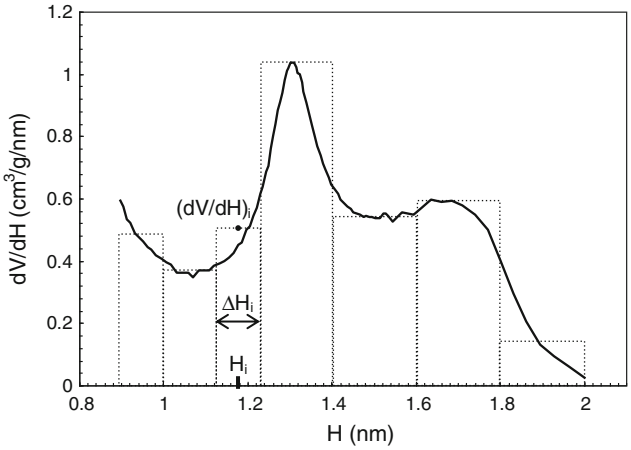

Fig. 1 Ecosorb PSD and its discretization

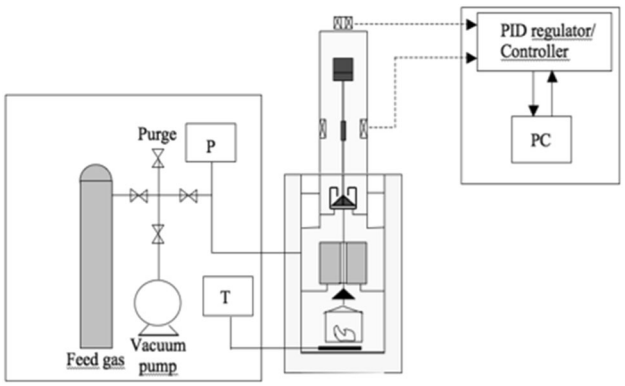

Fig. 2 Experimental set-up

As shown in the figure, the experimental device consists of a crucible hanging from a permanent magnet by a coupling system. The permanent magnet is kept suspended by the effect of an electromagnet. The force due to the mass uptake during the adsorption process is transmitted to the analytical balance by the magnetic suspension (coupling of the permanent magnet and electromagnet). The position of the permanent magnet is kept constant by a regulation system, which detects the variation of its vertical position, and a PID controller, which regulates its position by changing the current circulating in the electromagnet.

Given the fact that the vertical position of the permanent magnet is constant, the force transmitted to the analytical balance is equal to the weight of the crucible-adsorbent-adsorbed phase system. The crucible, the coupling system, and the permanent magnet are located inside the adsorption chamber, where the adsorbate is introduced at the experimental temperature and pressure conditions.

During adsorption isotherms measurements, the balance is kept at a constant temperature by two heating jackets,

one for the adsorption chamber and another for the suspension coupling. The temperature is measured by a platinum resistance temperature sensor (Pt100) placed directly in the adsorption chamber, with an accuracy of 0.1 K. The pressure gauge was purchased from Wika with a sensitivity of 0.01 % of the full scale.

2.3 Experimental procedure

Prior to all operations, the sample is regenerated under vacuum ($<10^{-4}$ MPa) at 523.15 K (local heating system) for 24 h, using a diffusion pump.

Successive amounts of adsorbate are then admitted inside the adsorption chamber. After each admission, and once equilibrium is reached, the pressure, temperature, and adsorbed mass are measured and recorded at regular intervals, and then a new amount of gas is admitted. The average time to obtain one adsorbed mass is 40 min.

2.3.1 Measuring principle

The measuring principle is based on the mechanical balance of forces acting on the system placed in the adsorption chamber. This balance allows different separate measurements: (i) in the so called "ZP position", the typing alone is lifted and weighed, (ii) in the called "MP1 position" both typing and crucible are suspended and weighed.

Considering that ZP and MP1 masses are directly read from the acquisition unit, we obtain the following equations:

$$ZP = m_t - \rho_{gas} V_t \quad (1)$$

where m_t and V_t denote the mass and volume of the typing and ρ_{gas} the gas density at (T,P).

$$MP1 = (m_t + m_c) - \rho_{gas}(V_t + V_c) \quad (2)$$

where m_c and V_c denote the mass and volume of the crucible.

The amount of material adsorbed is determined by placing a substrate (or adsorbent) in the crucible. Using the previous equations, the adsorbed mass of gas on the surface of the substrate m_{ads} is expressed as follows:

$$m_{ads} = (MP1-ZP) + \rho_{gas}(V_c + V_{adsorbent} + V_{adsorbed}) - (m_c + m_{adsorbent}) \quad (3)$$

However, it is impossible to determine experimentally the volume of the adsorbed phase. Therefore, the only available variable is the excess mass, m_{ex}, defined as:

$$m_{ex} = m_{ads} - \rho_{gas} V_{adsorbed} = (MP1-ZP) + \rho_{gas}(V_c + V_{adsorbent}) - (m_c + m_{adsorbent}) \quad (4)$$

2.3.2 Calibration with helium

As described before, measuring the adsorbed excess amount entails the knowledge of four terms. The first one, (MP1–ZP), is obtained by simple difference of the signal values read from the positions MP1 and ZP. The gas density can be deduced from any available dedicated equation of state, with high accuracy in the case of simple gases as methane. The two characteristic variables of the crucible and the adsorbent (m_c,$m_{adsorbent}$,V_c,$V_{adsorbent}$) are deduced from a helium calibration procedure (helium is used for this step because it is considered not to be adsorbed). The plot of the linear function (MP1–ZP) = $f(\rho_{He})$ (changing the pressure under isothermal conditions) allows to determine ($m_c + m_{adsorbent}$) and ($V_c + V_{adsorbent}$). An example of the helium calibration results obtained in this work is shown in Fig. 3.

2.3.3 Measurement accuracy

The uncertainty in determining the excess adsorbed mass results from the addition of the uncertainties affecting each term of Eq. (4).

$$\Delta m_{ex} = \Delta(MP1) + \Delta(ZP) + (V_c + V_{adsorbent})\Delta\rho + \rho\Delta(V_c + V_{adsorbent}) + \Delta(m_c + m_{adsorbent}) \quad (5)$$

The uncertainty in the ZP term is directly related to the accuracy of the balance, i.e. ±10 µg, while the uncertainty in the MP1 term is related to the stability of the system during a measurement of the adsorbed amount. The latter is deduced from a stability criterion estimated to be ±80 µg (Ghoufi et al. 2009). The error made on the estimation of the characteristics of the system $\Delta(m_c + m_{adsorbent})$ and $\Delta(V_c + V_{adsorbent})$ comes from the accuracy on the

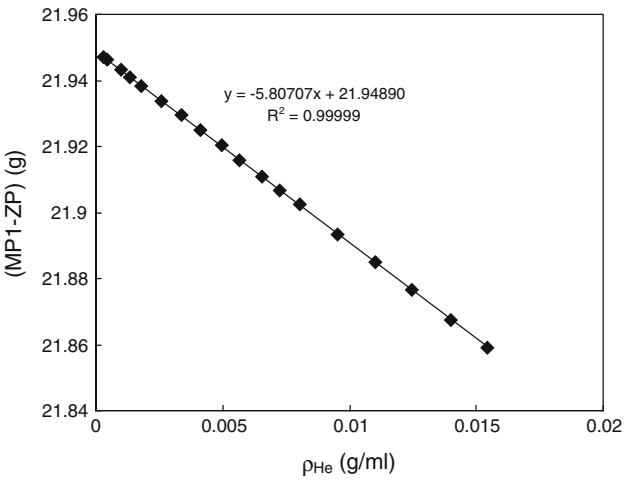

Fig. 3 Results of helium calibration procedure

calibration with helium. A calculation of uncertainty leads to the following results: $\Delta(V_c + V_{adsorbent}) = \pm 0.01$ cm^3 and $\Delta(m_c + m_{adsorbent}) = \pm 20$ μg

The relative uncertainty concerning the gas density value determined using a specific equation of state is lower than 0.05 % (Setzmann and Wagner 1991). Errors induced by the uncertainties of temperature and pressure are negligible. Finally, the overall uncertainty on the determination of the excess adsorbed mass is determined to be lower than 1 % over the entire range investigated in this study.

3 Monte Carlo simulation procedure

The most widely used ensemble in the Monte Carlo molecular simulation of adsorption in confined porous media is the Grand Canonical ensemble. This technique allows computing directly the equilibrium between a gas phase in an external reservoir in contact with the adsorbed phase inside the pore, a situation where the chemical potential of the system is constant and equal to the bulk value for the experimental temperature and pressure conditions, but the pressure and number of molecules inside the pore are not constant, thus reproducing exactly the thermodynamic experimental conditions. Thus, in this ensemble the chemical potential μ of the fluid in the bulk phase where the pore is immersed, the internal volume of the pore and the temperature are the constant variables whose values are fixed a priori.

Considering the highly lamellar structure of activated carbons, their single pores are generally assumed to be slit-shaped. Hence, in this work it is assumed that the solid consists of slit-like pores represented by two semi-infinite parallel walls of graphite separated by a distance H, namely the pore width, standing for the distance between the nuclei of the carbon atoms of the first layer on opposing pore walls. A standard parallelepipedic simulation box is used to model the slit-shaped pore, with the confining walls placed at the top and bottom of it, while the usual periodic boundary conditions and minimum image convention hold in the x and y directions. The x and y dimensions of the simulation box were set in this work to 15 σ_{ff}; higher values were used for the smallest pores at the lowest pressures to ensure a sufficient amount of particles in the box.

The molecule of methane is modeled as a single Lennard–Jones (LJ) sphere. The LJ potential characteristic parameters used are those proposed by Möller et al. (1992), σ_{ff} = 3.7327 Å for the collision diameter and ε_{ff}/k = 149.92 K for the potential well depth. This molecular model, although very simple, has already proved to be efficient for methane adsorption modeling (Kowalczyk et al. 2005), in addition to the precise estimations provided also for demanding tests as response functions (Lagache et al. 2004, Bessières et al. 2006) or fluid–fluid interfacial properties (Miqueu et al. 2011).

The interaction between a methane molecule and each graphite wall is modeled by the well-known Steele's potential (Steele 1973):

$$V_{sf}(z) = 2\pi\varepsilon_{sf}\rho_S\sigma_{sf}^2\Delta\left[\frac{4}{10}\left(\frac{\sigma_{sf}}{z}\right)^{10} - \left(\frac{\sigma_{sf}}{z}\right)^{4} - \frac{\sigma_{sf}^4}{3\Delta(z+0.61\Delta)^3}\right] \quad (6)$$

Although the graphite surface is made of carbon atoms arranged in a hexagonal structure, the Steele's potential has proved to work well for many substances including hydrocarbons (Steele 1973, Tan and Gubbins 1990). Steele's equation models the solid as a series of continuous lattice planes separated by a distance Δ. The first two terms result from the integration of the LJ potential over the x and y direction for the outermost graphite plane. The last term results from a summation over all the other planes with the assumption that the repulsive part can be neglected. The parameters modeling the graphite surface are taken from Tan and Gubbins (1990): σ_{ss} = 3.4 Å, ε_{ss}/k = 28 K, the number of carbon atoms per unit volume of graphite is ρ_s = 114 nm^{-3} and the separation between the graphite layers is Δ = 3.35 Å.

The solid–fluid molecular parameters are estimated from the classical Lorentz–Berthelot mixing rules: $\sigma_{sf} = \frac{1}{2}(\sigma_s + \sigma_f)$ and $\varepsilon_{sf} = \sqrt{\varepsilon_s\varepsilon_f}$, without computing any type of additional crossed interaction parameters.

The external potential experienced by a molecule within the fluid placed at a position with coordinates (x, y, z) is the sum of V_{sf} for the two interacting walls:

$$V_{ext}(z) = V_{sf}(z) + V_{sf}(H - z) \quad (7)$$

The chemical potential has been previously calculated during an isothermal-isobaric (NPT) bulk simulation run at the experimental P and T values, using the Widom insertion test method to determine the chemical potential, and this value was used later to fix the chemical potential inside the pore for the GCMC simulation (Ungerer 2005). The GCMC simulations involved attempts to move, create or destroy a molecule with equal probability. The system was equilibrated during 10^7–10^9 configurations. After equilibration the overall density in the pore was determined by averaging about 10^8–10^9 configurations, depending on the pore size and pressure. The average number of methane molecules varied between 100 and 1,000, depending also on the pore size and pressure.

3.1 Adsorption isotherm

The actual quantity calculated in the GCMC simulations is the average number of molecules in each pore. For comparison with experimental data, which represent excess adsorption, the simulated values need to be corrected. Various definitions are currently used for adsorption: total, excess, per unit wall area, and per unit pore volume, with different definitions of pore width. In this work, we have used a definition of the excess adsorption for each pore that is consistent with the experimental excess adsorption:

$$\Gamma_i = \int_0^{H_i} \rho(z)dz - \rho_{bulk} H_{i,He} \tag{8}$$

This definition mimics the experimental calibration procedure in order to make the theory and the experiment entirely consistent. $H_{i,He}$ is the width of the effective slit-shaped pore having the "Helium calibrated" pore volume determined through molecular simulation as a previous calculation step, according to $H_{He} = H_i - 2 \times 0.71 \times \frac{\sigma_s + \sigma_{He}}{2}$ where σ_{He} = 2.6 Å.

This definition was first proposed by Neimark and Ravikovitch (1997) and mimics the experimental helium calibration procedure, in order to determine precisely the pore accessible volume, making theory and experiment entirely consistent.

Neimark and Ravikovitch (1997) confirmed that the discrepancy between the helium pore width and the geometrical internal pore dimensions is not negligible for micropores and thus, the use of a equation for Γ_i different than Eq. (8) can lead to large discrepancies between MC simulations and experiments.

In order to compute the adsorption for the whole system, the contribution of each pore size must be accounted for by using the information obtained for the experimental PSD. Then,

$$n_{ex}(P) = \sum_i \Gamma_i \left(\frac{dV}{dH}\right)_i \frac{\Delta H_i}{H_i} \tag{9}$$

where $n_{ex}(P)$ is the excess adsorbed amount per mass of substrate, $\left(\frac{dV}{dH}\right)_i$ is the discrete analogue of the PSD and ΔH_i is the discretization step size (see Fig. 1).

3.2 Heat of adsorption

The isosteric heat of adsorption corresponds to the enthalpy change on transferring a molecule of adsorbate from the gas to the adsorbed phase at constant pressure. The calculation of the heat of adsorption by molecular simulation is well established for a single pore (Do et al. 2007) and is calculated directly using fluctuation theory:

$$Q_{st} = kT - \frac{\langle N\,U\rangle - \langle N\rangle\langle U\rangle}{\langle N^2\rangle - \langle N\rangle^2} \tag{10}$$

where N is the total number of particles in the pore and U is the total configurational energy of the fluid within the pore. This equation is used to compute the contribution of each pore to the heat of adsorption. As explained by Birkett and Do (2006), the calculation of isosteric heat of adsorption for a heterogeneous solid using individual heats calculated for every single pore size has been often treated in a wrong way. In their work, Birkett and Do (2006) demonstrate the following expression for the total Q_{st} obtained from the PSD $\left(\frac{dV}{dH}\right)$and the contribution of each pore:

$$Q_{st}(P) = \frac{\int_0^\infty Q_{st}(P,H)\left(\frac{\partial\rho}{\partial P}\right)_{T,V}\frac{dV}{dH}(H)\,dH}{\left(\frac{\partial N_{tot}(P)}{\partial P}\right)_{T,V}} \tag{11}$$

where $\rho(H,P)$ is the density in a pore of width H and $N_{tot} = \int_0^\infty \rho(H,P)\,\frac{dV}{dH}(H)\,dH$ is the absolute amount adsorbed in the porous media. For practical use, the integral in N_{tot} is replaced by the sum over discrete intervals using the PSD given in Fig. 1.

The actual heat of adsorption measured with the calorimetric device is the differential heat of adsorption Q_{dif}. Hence, for comparison with measured values, the differential heat of adsorption Q_{dif} was computed with

$$Q_{dif} = Q_{st} - RT \tag{12}$$

with Q_{st} obtained with Eq. (11).

4 Results and discussion

A series of local density profiles were collected by GCMC for the pore size and pressure ranges concerned by the experimental study of Ecosorb. They have served first to gain insight into the supercritical methane adsorption behavior and then to compute the adsorption isotherms and isosteric heat of adsorption and compare them to the measured values.

As an example, Fig. 4 represents the average density $\langle\rho\rangle$ of methane at 303 K obtained from GCMC calculations for a series of slit like micropores from nearly 0.1 to 8 MPa. As expected the net adsorbed amount of methane in a pore increases with pressure. Oscillations of the adsorption with increasing pore width are related to the fact that molecules achieve the highest density when they fill completely an integer number of layers. The methane molecules tend to form ordered layering structures due to the presence of the confining wall, which is a clear and well-known effect of the so-called surface ordering or anchoring. Thus, some pore sizes are favorable to perfect packing (maximum of

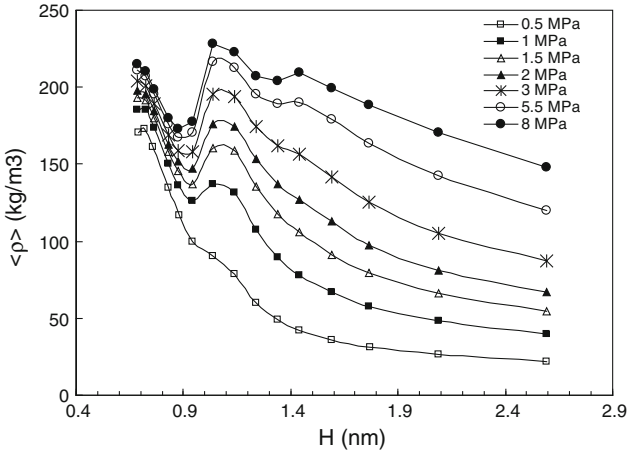

Fig. 4 Average density of methane versus pore size at 303 K obtained from GCMC calculations

$\langle\rho\rangle$) and others cause unfilled voids (minimum of $\langle\rho\rangle$). When pores become larger, such oscillations rapidly vanish. All these features mentioned above are of course in agreement with previous published works (Tan and Gubbins 1990, Olivier 1998, Davies and Seaton 1998, Nicholson 2002, Ustinov and Do 2003, Kowalczyk et al. 2005).

Adsorption isotherms for pure methane on Ecosorb activated carbon at 303.15 and 353.15 K and pressures up to 10 MPa are presented in Fig. 5. The amount of methane adsorbed n_{ex} is calculated as $n_{ex} = \frac{m_{ex}}{M_{gas} m_{adsorbent}}$. Equation (9) was used to compute the excess adsorbed quantity that mimic the experimental data thanks to the PSD of the activated carbon. This latter was obtained from the measurement of the N_2 adsorption isotherm at 77 K with a gas porosimeter (Micromeritics ASAP 2020) in combination with a homemade filling pressure model published previously (Malheiro et al., unpublished work). The Ecosorb PSD is plotted in Fig. 1, together with the discretization used in Eqs. (9) and (11). The excellent agreement between both sets of data in Fig. 5 proves the consistency of the methodology used in this work, from the characterization of the porous media in terms of PSD to the computational results through experimental isotherms determination. The agreement between the modeled and experimental isotherms shown in Fig. 5 is similar to the ones obtained on the one hand by Liu and Monson (2005) for methane on BPL activated carbon represented by a revised platelet model and on the other hand by Do et al. (2003) on graphitized thermal carbon black. Aukett et al. (1992) had obtained poorer results for the adsorption of supercritical methane on AX21 but this might be due to an improper PSD that seemed to overestimate the pore volume, which emphasizes the importance of a "good" PSD in the modeling of isotherm adsorption.

In order to complete the comparison between simulations and experiments with the additional support of an energetic thermodynamic magnitude, the isosteric heat of adsorption was computed with Eq. (10) for the series of pores and pressures of interest here, and the results are presented in Fig. 6. As shown, the dependence of heat of adsorption with pressure is weak. For a given pore size, the heat of adsorption increases with pressure from the lowest pressure range to become nearly constant when pressure is higher than 2 MPa approximately. As for the average pore density, the variation of Q_{st} with pore size is oscillating with maxima appearing every time a supplementary layer can be accommodated inside the pore. The highest values of Q_{st} are achieved for the smallest pores. Indeed, for these pore sizes, the solid–fluid interactions are the highest because of the overlapping of the interactions of the opposite pore walls. The isosteric heat of adsorption has a maximum value when the pore size is $\sim$0.7 nm whatever

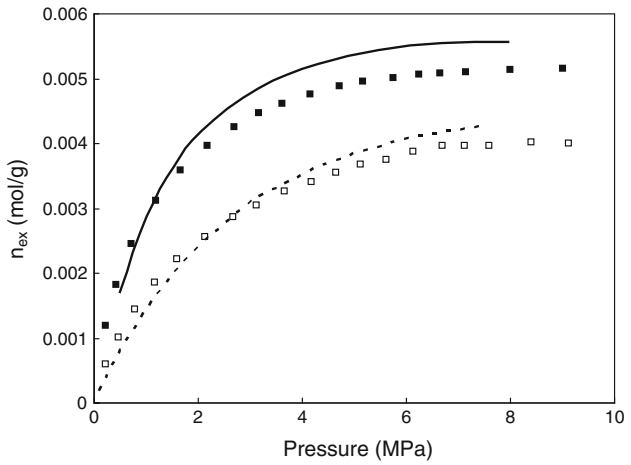

Fig. 5 Experimental methane adsorption isotherms at 303.15 K (*filled rectangle*) and at 353.15 K (*unfilled rectangle*)

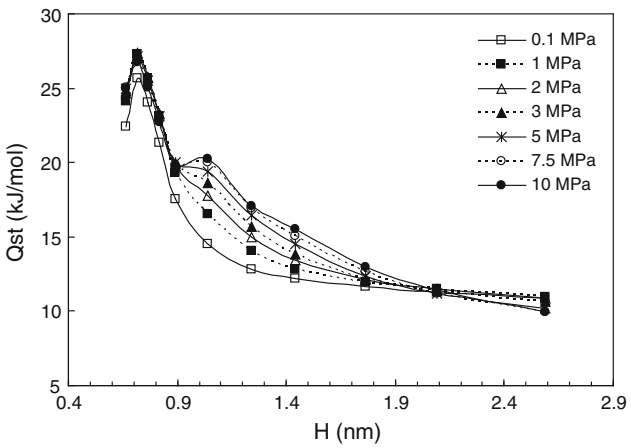

Fig. 6 Isosteric heat of adsorption versus pore size obtained from GCMC calculations

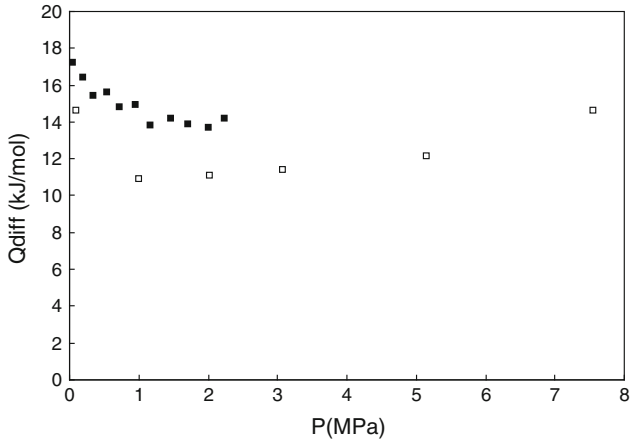

Fig. 7 Experimental and computed differential heat of adsorption at 353.15 K: exp (*filled rectangle*) and computed (*unfilled rectangle*)

the pressure. This result was previously obtained by Shindler and LeVan (2008) in the Henry's law region. Here, we show that this maximum exists also in the high pressure region at the same pore size.

Then, the differential heat of adsorption of methane on Ecosorb was computed at 353 K with Eqs. (11) and (12) and compared with experimental data provided by a manometric–calorimetric coupled apparatus (Mouahid et al. 2012). As illustrated in Fig. 7, comparison with these experiments shows that GCMC can be used for the determination of the energetic effects due to the adsorption phenomenon. Qualitatively, the trend of the two sets of data is very similar. Quantitatively computed values systematically underestimate the experimental ones. However, one has to keep in mind the uncertainties of both experimental and computed values. Indeed, as mentioned by Mouahid et al. (2012), the uncertainty in the experimental values is at least of 8 %. Concerning the simulated heats of adsorption, Levesque and Lamari (2009) have clearly shown the difficulty of estimating with a good accuracy the heat of adsorption of a macroscopic sample. Indeed, first of all, the statistical error for the heat of individual small micropores is important because the values of $\langle N^2 \rangle$ and $\langle N \rangle^2$ in Eq. (10) are similar for small micropores. Secondly, another uncertainty results from the derivatives with pressure in Eq. (11). Thus, the uncertainty in the simulated heats of adsorption represented in Fig. 7 should be regarded as not negligible with a value of at least 15 %.

5 Conclusion

In this paper the adsorption of pure methane in activated carbon Ecosorb was studied by combining GCMC molecular simulation and an experimental approach based on a gravimetric device. The comparison between both experimental and estimated data proved the consistency of the methodology used in this work, starting from the characterization of the porous media in terms of PSD, the determination of the experimental adsorption isotherms, and the final estimation of computational results through experimental isotherms determination as well as the differential heat of adsorption. The combination of both experimental and computational homemade results allowed a complete characterization of the activated carbon substrate and its methane storage capacity.

Acknowledgments This work was sponsored by the *European Research Council* (ERC) advanced grant Failflow (27769). This financial support is gratefully acknowledged. MMP acknowledges financial support from Ministerio de Economía y Competitividad (Spain), through project ref. FIS2012-33621, co-financed with EU FEDER funds.

References

Abdul Razak, M., Do, D.D., Horikawa, T., Tsuji, K., Nicholson, D.: On the description of isotherms of CH_4 and C_2H_4 adsorption on graphite from subcritical to supercritical conditions. Adsorption **19**, 131–142 (2013)

Aukett, P.N., Quirke, N., Riddiford, S., Tennison, S.R.: Methane adsorption on microporous carbons—a comparison of experiment, theory, and simulation. Carbon **30**(6), 913–924 (1992)

Bessières, D., Randzio, S.L., Piñeiro, M.M., Lafitte, Th, Daridon, J.-L.: A combined pressure-controlled scanning calorimetry and monte carlo determination of the Joule–Thomson inversion curve. Application to methane. J. Phys. Chem. B **110**, 5659–5664 (2006)

Birkett, G.R., Do, D.D.: Correct procedures for the calculation of heats of adsorption for heterogeneous adsorbents from molecular simulation. Langmuir **22**(24), 9976–9981 (2006)

Chen, X.S., McEnaney, B., Mays, T.J., Alcaniz-Monge, J., Cazorla-Amoros, D., Linares-Solano, A.: Theoretical and experimental studies of methane adsorption on microporous carbons. Carbon **35**(9), 1251–1258 (1997)

Cracknell, R.F., Gordon, P., Gubbins, K.E.: Influence of pore geometry on the design of microporous materials for methane storage. J. Phys. Chem. **97**(2), 494–499 (1993)

Davies, G.M., Seaton, N.A.: The effect of the choice of pore model on the characterization of the internal structure of microporous carbons using pore size distributions. Carbon **36**(10), 1473–1490 (1998)

Do, D.D., Do, H.D., Ustinov, E.: Adsorption of supercritical fluids on graphitised thermal carbon black: molecular layer structure theory versus grand canonical Monte Carlo simulation. Langmuir **19**, 2215–2225 (2003)

Do, D.D., Nicholson, D., Do, H.D.: Heat of adsorption and density distribution in slit pores with defective walls: GCMC simulation studies and comparison with experimental data. Appl. Surf. Sci. **253**(13), 5580–5586 (2007)

Ghoufi, A., Gaberova, L., Rouquerol, J., Vincent, D., Llewellyn, P.L., Maurin, G.: Adsorption of CO_2, CH_4 and their binary mixture in Faujasite NaY: a combination of molecular simulations with gravimetry-manometry and microcalorimetry measurements. Microporous Mesoporous Mater. **119**(1–3), 117–128 (2009)

Kowalczyk, P., Tanaka, H., Kaneko, K., Terzyk, A.P., Do, D.D.: Grand canonical Monte Carlo simulation study of methane

adsorption at an open graphite surface and in slitlike carbon pores at 273 K. Langmuir **21**, 5639–5646 (2005)

Lagache, M.H., Ungerer, Ph, Boutin, A.: Prediction of thermodynamic derivative properties of natural condensate gases at high pressure by Monte Carlo simulation. Fluid Phase Equilib. **220**(2), 211–223 (2004)

Levesque, D., Lamari, F.D.: Pore geometry and isosteric heat: an analysis of carbon dioxide adsorption on activated carbon. Mol. Phys. **107**(4–6), 591–597 (2009)

Liu, J.-C., Monson, P.A.: Molecular modeling of adsorption in activated carbon: comparison of Monte Carlo simulations with experiment. Adsorption **11**(1), 5–13 (2005)

Lozano-Castelló, D., Cazorla-Amorós, D., Linares-Solano, A., Quinn, D.F.: Activated carbon monoliths for methane storage: influence of binder. Carbon **40**(15), 2817–2825 (2002a)

Lozano-Castelló, D., Cazorla-Amorós, D., Linares-Solano, A., Quinn, D.F.: Influence of pore size distribution on methane storage at relatively low pressure: preparation of activated carbon with optimum pore size. Carbon **40**(7), 989–1002 (2002b)

MacDonald, J.A.F., Quinn, D.F.: The preparation of active carbons from natural materials for use in gas storage. J. Porous Mater. **1**(1), 43–54 (1995)

Malheiro, C., Mendiboure, B., Plantier, F., Guatarbes, B., Miqueu, C.: An accurate model for the filling pressure of carbon slit-like micropores. Application to the pore size distribution calculation (2014)

Matranga, K.R., Myers, A.L., Glandt, E.D.: Storage of natural gas by adsorption on activated carbon. Chem. Eng. Sci. **47**(7), 1569–1579 (1992)

Miqueu, C., Míguez, J.M., Piñeiro, M.M., Lafitte, Th, Mendiboure, B.: Simultaneous application of the gradient theory and Monte Carlo molecular simulation for the investigation of methane/water interfacial properties. J. Phys. Chem. B **115**(31), 9618–9625 (2011)

Möller, D., Oprzynski, J., Muller, A., Fischer, J.: Prediction of thermodynamic properties of fluid mixtures by molecular dynamics simulations: methane-ethane. Mol. Phys. **75**(2), 363 (1992)

Mouahid, A., Bessieres, D., Plantier, F., Pijaudier-Cabot, G.: A thermostated coupled apparatus for the simultaneous determination of adsorption isotherms and differential enthalpies of adsorption at high pressure and high temperature. J. Therm. Anal. Calorim. **109**(2), 1077–1087 (2012)

Neimark, A.V., Ravikovitch, P.I.: Calibration of pore volume in adsorption experiments and theoretical models. Langmuir **13**, 5148–5160 (1997)

Nicholson, D.: A simulation study of the pore size dependence of transport selectivity in cylindrical pores. Mol. Phys. **100**(13), 2151–2163 (2002)

Olivier, J.P.: Improving the models used for calculating the size distribution of micropore volume of activated carbons from adsorption data. Carbon **36**(10), 1469–1472 (1998)

Quinn, D.F., Ragan, S.: Carbons suitable for medium pressure (6.9 MPa) methane storage. Adsorpt. Sci. Technol. **18**(6), 515–527 (2000)

Santillán-Reyes, G.G., Pfeiffer, H.: Analysis of the CO_2 capture in sodium zirconate (Na_2ZrO_3). Effect of the water vapor addition. Int. J. Greenh. Gas Control **5**(6), 1624–1629 (2011)

Schindler, B.J., LeVan, M.D.: The theoretical maximum isosteric heat of adsorption in the Henry's law region for slit shaped carbon nanopores. Carbon **46**, 644–648 (2008)

Setzmann, U., Wagner, W.: A new equation of state and tables of thermodynamic properties for methane covering the range from the melting line to 625 K at pressures up to 1000 MPa. J. Phys. Chem. Ref. Data **20**(6), 1061–1151 (1991)

Steele, W.A.: The physical interaction of gases with crystalline solids. I. Gas–solid energies and properties of isolated adsorbed atoms. Surf. Sci. **36**(1), 317–352 (1973)

Tan, Z., Gubbins, K.E.: Adsorption in carbon micropores at supercritical temperatures. J. Phys. Chem. **94**(15), 6061–6069 (1990)

Ungerer, P., Tavitian, B., Boutin, A.: Applications of Molecular Simulation in the Oil and Gas Industry: Monte Carlo Methods. Editions Technip, Paris (2005)

Ustinov, E.A., Do, D.D.: High-pressure adsorption of supercritical gases on activated carbons: An improved approach based on the density functional theory and the bender equation of state. Langmuir **19**(20), 8349–8357 (2003)

Yang, Z., Xia, Y., Zhu, Y.: Preparation and gases storage capacities of N-doped porous activated carbon materials derived from mesoporous polymer. Mater. Chem. Phys. **141**(1), 318–323 (2013)

Zhou, F., Hussain, F., Cinar, Y.: Injecting pure N_2 and CO_2 to coal for enhanced coalbed methane: experimental observations and numerical simulation. Int. J. Coal Geol. **116–117**, 53–62 (2013)